Supramolecular Chemistry |*Hot Paper*|

Oligo-Quinolylene–Vinylene Foldamers

Jinhua Wang,[a] Barbara Wicher,[b] Victor Maurizot,*[a] and Ivan Huc*[a, c]

Abstract: Quinoline based aromatic amide foldamers are known to adopt stable folded conformations. We have developed a synthetic approach to produce similar oligomers where all amide bonds, or part of them, have been replaced by an isosteric vinylene group. The results of solution and solid state structural studies show that oligomers exclusively containing vinylene linkages are not well folded, and adopt predominantly flat conformations. In contrast, a vinylene segment flanked by helical oligoamides also folds in a helix, albeit with a slightly lower curvature. The presence of vinylene functions also result in an extension of π-conjugation across the oligomer that may change charge transport properties. Altogether, these results pave the way to foldamers in which both structural control and specific electronic properties may be engineered.

Introduction

Isosteres are molecules or functional groups that possess similar overall morphologies. The use of isosteric replacement is well known and used in medicinal chemistry to improve small molecule drug design by modulating their activity, degradability and facilitating their synthetic access.[1] Isosteric replacement has also been demonstrated in biomolecules such as peptides.[2] The isosteric replacement of an amide group has been used to probe peptide structure[3] as well as function.[4] Peptide isosteres have been shown to resist enzyme degradation which enhances their suitability for therapeutic applications.[5] Among various possible peptide backbone modifications, the vinyl group has been one of the most studied amide surrogates to date, due to its similarities in shape, bond lengths and bond angles.[6]

Aside from isosteres, biomolecular mimicry has been demonstrated through the use of entirely synthetic, unnatural building blocks. These may not necessarily perfectly match the shape of a parent macromolecule, but they fold into architectures that overall resemble biopolymer secondary structures such as helices or sheets found in proteins.[7] Along this line, our group[8] and others[9] have developed aromatic oligoamide foldamers (AOFs). In AOFs, the amide group serves both easy synthetic accessibility and mediates intramolecular non covalent interactions that induce conformational restrictions eventually leading to folding. Among the different families of AOFs, oligoamides of 8-amino-2-quinolinecarboxylic acid have been extensively studied (Scheme 1).[10] In these molecules, pseudo-conjugation between contiguous amide and aryl sp^2 groups favors co-planarity. Furthermore, local electrostatic NH···N attractions and C=O···N repulsions involving the amide groups and neighboring quinoline endocyclic nitrogen atoms have been shown to be responsible for a strong conformational bias at rotatable bonds,[11] resulting in strand curvature and eventually promoting helical folding. In the helix, contacts between stacked aromatic rings further stabilize the structure, in particular in protic solvents.[10c] These molecules have been previously shown to work as peptide or DNA mimics and to interact

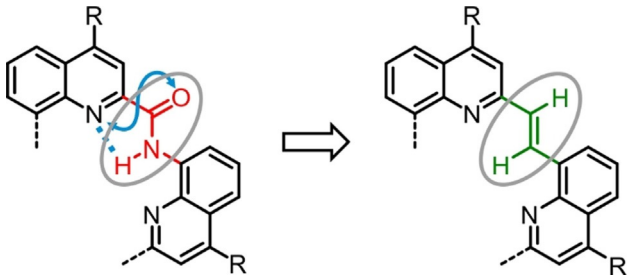

Scheme 1. Amide linkage and its vinyl isostere in a quinoline oligomer. The double-headed arrow shows electrostatic repulsions.

[a] *J. Wang, Dr. V. Maurizot, Prof. I. Huc*
CBMN (UMR5248), Univ. Bordeaux–CNRS–IPB
Institut Européen de Chimie et Biologie, 2 rue Escarpit
33600 Pessac (France)
E-mail: victor.maurizot@u-bordeaux.fr

[b] *Dr. B. Wicher*
Department of Chemical Technology of Drugs
Poznan University of Medical Sciences, Grunwaldzka 6
60-780 Poznan (Poland)

[c] *Prof. I. Huc*
Department of Pharmacy and Cluster e-conversion
Ludwig-Maximilians-Universiät, Butenandtstrasse 5–13
81377 München (Germany)
E-mail: ivan.huc@cup.lmu.de

Supporting information and the ORCID identification number(s) for the author(s) of this article can be found under: https://doi.org/10.1002/chem.202003559.

with proteins.[8c,12] Furthermore, they have also been shown to possess remarkable charge transport properties, through both photo-induced charge transfer between a donor and an acceptor group placed at the extremities of a helix, and at metal–organic–metal junctions.[13] Charge transport is thought to proceed via a hopping mechanism, whereby an electron hops, generating a quinoline radical cation that propagates along the helical structure. Theoretical calculations suggested that the efficiency of hole transport, that is, the low attenuation of charge transport rates with distance, was a result of the coexistence of two pathways, one through the pseudo-conjugated amide backbone, the other along the helical axis through stacked quinoline rings.[13]

In the interest of further improving the charge transport properties of aromatic foldamer helices, we considered replacing some amide groups of quinoline-based helical AOFs with vinyl groups. Indeed, the vinyl group is not only a commonly encountered amide isostere but it is also a promoter of conjugation between contiguous aryl rings. Poly(*p*-phenylene-vinylene) is a semiconducting polymer[14] and large π-conjugated compounds have been extensively studied in the field of optoelectronic organic materials.[14a,15] Nevertheless, despite its common use in polymeric materials, the vinyl group has rarely been exploited in aliphatic[16] and aromatic[17] foldamer main chains. Replacing amides by vinyl groups in AOFs obviously introduces additional degrees of conformational freedom as aforementioned hydrogen bonding and electrostatic repulsions no longer occur. It was thus not clear at the start of this study whether, and under which condition, the vinyl-containing AOFs oligomers would fold.

Herein, we present an efficient synthesis of quinolylene–vinylene oligomers and of hybrid sequences with AOFs. We show that quinolylene–vinylene oligomers do not possess a strong inherent folding propensity, but that they adopt helical conformations in a solvent dependent manner when flanked with helical AOF segments. These results pave the way to foldamers in which both structural control and specific electronic properties may be engineered.

Results and Discussion

Synthesis of homomeric quinolylene–vinylene oligomers

In order to evaluate the structural influences of vinyl linkages in quinoline-based foldamers, a series of organic soluble oligomers (**6**–**11**) composed of 2 to 7 quinoline units were prepared and their propensity to fold into defined architectures was studied in solution using ^{1}H NMR spectroscopy and in the solid state via X-ray crystallography. The synthesis was achieved according to the route described in Scheme 2 (see Supporting Information for details). The synthetic strategy is based on the iterative addition of one monomer at a time to the oligomer through a Horner–Wadsworth–Emmons (HWE) olefination using phosphonate ester **5** as the key building block. The elongation of the oligomer was implemented at the terminal carboxylate ester, through its conversion to the corresponding aldehyde and through a subsequent HWE reaction with **5**. A

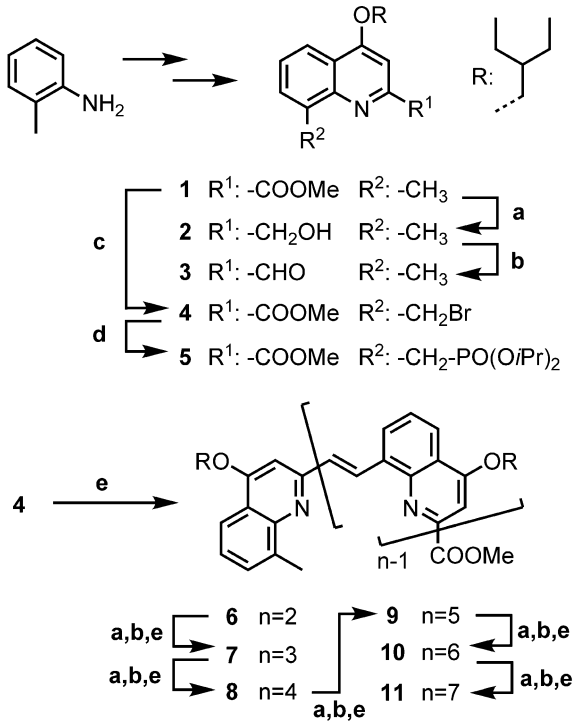

Scheme 2. Synthesis of quinolylene–vinylene oligomers. a: $NaBH_4$, THF, 60 °C; b: SIBX, THF, 60 °C; c: *N*-bromosuccinimide (NBS), CCl_4, rfx; d: $P(OiPr)_3$; e: i) **5**, NaH, 15-crown-5, THF; ii) MeI, K_2CO_3, Acetone.

direct reduction of the ester to the aldehyde using common reducing agents, such as DIBAL, was found to be hard to control and reproduce. Instead, a two-step pathway involving a quantitative reduction to the alcohol and a controlled re-oxidation using SIBX[18] afforded the aldehyde in good yield and high reproducibility.

The quinoline derivative **1** is both the starting monomer for chain elongation and a precursor of phosphonate ester **5**. It was prepared following similar procedures to those used in related AOF series.[19] The Michael addition of *o*-toluidine to dimethyl acetylene dicarboxylate gave a fumarate that was subsequently cyclized to produce a 4-(1*H*)-quinolone precursor of **1**. Alkylation using the Mitsunobu reaction with 2-ethyl-1-butanol afforded **1** which could then be converted in two steps to aldehyde **3**. Compound **1** was also converted in two steps to building block **5** after a radical bromination (using NBS as bromine source) and installation of the phosphonate group (Scheme 2). The subsequent HWE reaction between aldehyde **3** and phosphonate **5** using NaH as the base afforded the first vinyl group in the sequence. Only the *E* isomer was detected, as expected for a bulky phosphonate intermediate.[20] The *Z* isomer, if present at all, was not identified. Under the conditions used, partial saponification of the methyl ester occurred as an unwanted side reaction. Thus, an additional esterification step was performed as part of the work up to obtain the desired dimer **6** in 63% isolated yield. Oligomer elongation was then achieved by iterative conversion of the terminal methyl ester into an aldehyde followed by the addition of monomer **5** under optimized conditions. Oligomers **6**–**11**, composed of 2

to 7 quinoline units linked by 1 to 6 vinyl bonds, respectively, were obtained using this strategy. The yield per monomer elongation eventually decreased from 63% to 37%.

Structural investigation of homomeric quinolylene–vinylene oligomers

The UV/Vis spectra of monomer **1** and oligomers **6**–**11** were recorded in $CHCl_3$ (Figure S1) and highlighted that the introduction of one double bond (i.e. from **1** to **6**) resulted in bathochromic and hyperchromic shifts representative of a conjugated system. Further increase of the oligomer chain length (from **6** to **11**) resulted in a moderate but continuous red shift of the absorption maximum up to 430 nm. Fluorescence emission spectra demonstrated a similar red shift of the fluorescence emission maxima upon increasing oligomer length (Table S1), again reflecting the overall increase in the conjugation of π electron orbitals.

The folding propensity of these new oligomers was studied in solution by ^{1}H NMR spectroscopy in $CDCl_3$. In the parent AOFs, aromatic stacking associated with helical folding results in strong intramolecular ring current effects. Signals spread over a wide range of chemical shift values despite the repetitive nature of the sequence, and shift upfield as oligomer length increases.[8a,10a] This effect can be monitored, for example, by following the signal of the terminal methyl ester protons. The ^{1}H NMR spectra of quinolylene–vinylene oligomers **6**–**11** and of monomer **1** (Figure 1) show a degree of spreading of the chemical shift values and notably downfield shifted vinyl resonances in the 9.0-9.5 ppm range, presumably due to the deshielding effects of adjacent quinoline nitrogen atoms. The signal of the terminal methyl ester protons has the same chemical shift in the monomer **1** and the dimer **6**. However, in trimer **7**, it is upfield-shifted by 0.4 ppm, indicating a significant modification of the electronic environment of these protons attributed to overlapping aromatic rings. In a helical conformation, such an effect would be expected to increase upon oligomer elongation. In accordance with this, the signal is further upfield-shifted in tetramer **8**. However, this effect then plateaus, and a downfield shift is eventually observed when going from tetramer **8** to pentamer **9**. The ^{1}H NMR spectra are thus suggestive of folding but do not compare to what has been observed in parent AOFs.[10a] In addition, the sharp peaks and the absence of anisochronous AB patterns of the side chain methylene signals indicate that asymmetric conformations, if they exist, interconvert rapidly on the NMR time scale.

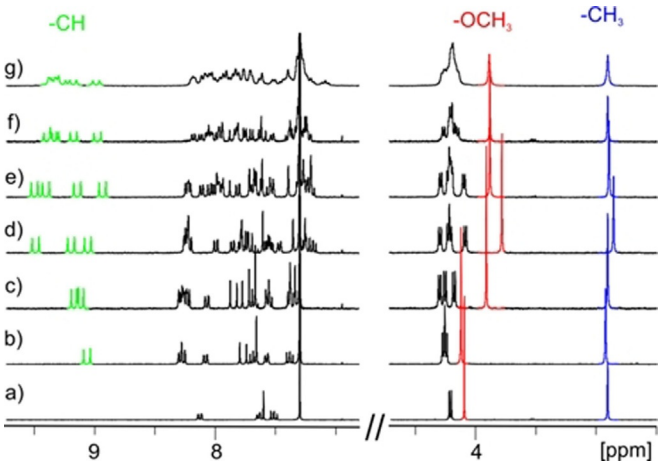

Figure 1. Part of the ^{1}H NMR spectra (300 MHz) of **1** and **6**–**11** at 298 K in $CDCl_3$: a) **1**; b) **6**; c) **7**; d) **8**; e) **9**; f) **10**; g) **11**. Methyl ester, terminal arylmethyl and vinyl proton signals are highlighted for all spectra in red, blue and green, respectively.

In order to investigate possible preferred conformations at aryl-vinyl linkages, ^{1}H-^{1}H-NOESY experiments were carried out in $CDCl_3$. Dimer **6** which contains a single vinyl group was used as the initial model. For this compound, four possible conjugated (flat) conformations may be considered by subsequent flips around aryl-vinyl bonds (I-IV in Figure 2a). Among them, conformers II and IV, when iterated in a long oligomer, would be conducive to helical folding whereas conformers I and III would result in flat tape structures.

For each of these conformations different sets of NOE correlations between aromatic protons H^3, H^7 and vinylic protons H^α, H^β are expected (Figure 2b). After assignment of the different signals, NOESY experiments performed with **6** demonstrated strong correlations between H^3 with H^α, and between H^7 and H^β, in agreement with conformer III (Figure 2c). However, weaker H^3–H^β and H^7–H^α correlations were also observed, suggesting that either conformer I, or II and IV, or I and II and IV, are also present. In short, conformational bias appears not to be quantitative and not conducive of a helical conformation. In order to assess whether cooperative effects associated with an increasing oligomer length change conformational behavior, NOESY experiments were also carried out on tetramer **8**, which contains four vinyl bonds (Figure S2). The pattern of correlations was found to be similar to that of dimer **6** indicating that flat conformations prevail.

In contrast with the solution behavior, a solid state structure of dimer **6** in its conformer II was obtained by crystallographic analysis of a single crystal grown by slow diffusion of methanol into a dichloromethane solution (Figure 2d). The structure is almost flat with a dihedral angle between the two aromatic rings of only 8.6°. The presence of this conformer in the solid makes it likely that its proportion in solution is not negligible.

In summary, homomeric quinolylene–vinylene oligomers appear not to adopt well defined conformations in solution. Tape-like conformations and bent helical conformations may coexist, perhaps even within the same molecule, and interconvert rapidly. A plausible approach to bias these conformational equilibria, and favor helical conformations, would be to investigate these molecules in protic solvent where solvophobic effects will disfavor tape conformations in which aryl rings are exposed. Such solvent induced folding has been evidenced in other aromatic oligomers.[21] Indeed, the addition of up to 40% CD_3OD to a $CDCl_3$ solution of hexamer **10** resulted in a spreading of aromatic and vinylic ^{1}H NMR signals over a larger range of chemical shifts and to some upfield shifts (Figure S3). The signals remained sharp. Such changes hint at an enhancement of ring current effects due to aromatic stacking, possibly associated with an enrichment of helical conformations. However,

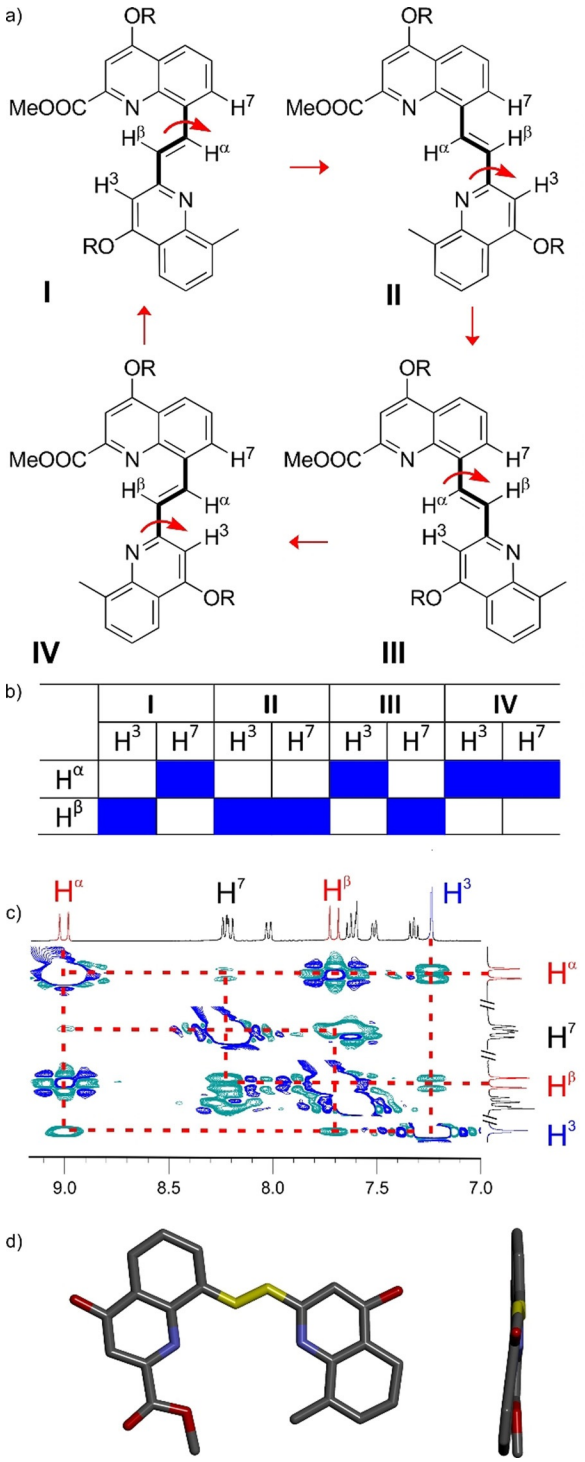

Figure 2. a) Four possible conformations of dimer **6**. b) Expected corresponding ^{1}H–^{1}H NOESY correlations. c) Part of the ^{1}H–^{1}H NOESY spectrum of **6** in $CDCl_3$ at 298 K (400 MHz) showing the correlations between vinyl protons and adjacent aromatic protons. d) Top (left) and side (right) views of the solid state structure of dimer **6**. All side chains and hydrogen atoms are removed for clarity; the vinylene group is highlighted in yellow.

hexamer **10** was not soluble beyond 40% CD_3OD. A full investigation of the effect of solvophobicity would entail the synthesis of a new family of oligomers bearing suitable solubilizing side chains in place of the 2-ethyl-butyloxy groups of **6**–**11**. This was not considered in the context of the current study. It was decided instead to investigate the effects of helical AOFs flanking quinolylene–vinylene segments.

Synthesis of hybrid quinolylene–vinylene quinolinecarboxamide oligomers

We have shown in earlier studies that helical AOFs can template the folding of otherwise flexible monomers.[22] In order to take advantage of this effect and dictate the folding of oligoquinolylene–vinylene segments into a helix, oligoamide precursors have been attached at the extremities of oligomers containing 1, 3, and 5 vinyl groups. Typically, tetrameric oligoamides were used, whose synthesis can be carried out on a multi-gram scale.[19] According to this design, oligomers **19**, **20** and **21** were prepared (Scheme 3).

The key building block for the synthesis of these hybrid oligomers is the Boc-amino-aldehyde **13**. This unit allows one to connect the oligoamide *C*-terminus to the oligo-quinolylene–vinylene segment, while the C-terminus of the latter can readily be coupled to the amine terminus of another oligoamide.

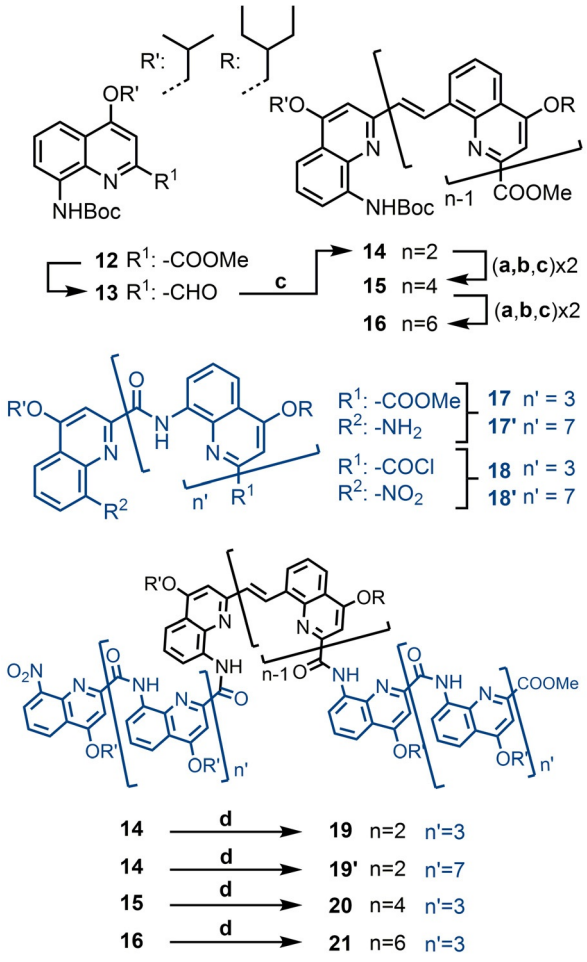

Scheme 3. Synthesis of quinoline oligoamide–oligovinylene hybrid foldamers. a: $NaBH_4$, THF, 60 °C; b: SIBX, THF, 60 °C; c: i) **5**, NaH, 15-crown-5, THF; ii) MeI, K_2CO_3, acetone; d: i) NaOH, THF/MeOH, RT; ii) $(COCl)_2$, CH_2Cl_2; iii) **17** or **17′**, iPr_2NEt, CH_2Cl_2; iv) TFA, $CHCl_3$; v) **18** or **18′**, iPr_2NEt, CH_2Cl_2.

Monomer **13** was prepared using a strategy similar to that of compound **1**. Boc-protected amino-ester **12** was reduced to its corresponding alcohol and re-oxidized to the desired aldehyde **13**. Subsequent elongation using a HWE reaction with the phosphonate ester **5**, followed by reduction of the carboxylate ester, similar to oligomers **6**–**11**, afforded the terminal BocNH-quinolylene–vinylene oligomers **14**, **15** and **16**, containing 1, 3, and 5 vinylene groups. Deprotection and coupling of tetrameric oligo-quinolinecarboxamide segments at each end led to the desired hybrids **19**–**21** containing vinylene segments of different lengths flanked by helically folded quinoline oligoamide tetramers.

Structural investigation of hybrid quinolylene–vinylene quinolinecarboxamide oligomers

The ^{1}H NMR analysis of hybrid oligomer **19** revealed the coexistence of two conformations (one major 91% and one minor 9%) in slow exchange on the NMR time scale (Figure 3a). Two sets of signals are observed in $CDCl_3$ at 298 K, the proportions of which do not depend on concentration but are dependent on solvent. Upon the addition of CD_3OH (Figure 3a) or upon replacing $CDCl_3$ by CD_2Cl_2 (Figure S10), the proportion of the minor species decreases further to less than 2%. By analogy with previous oligomers,[22] these two species were attributed to a PP/MM conformer where the two helical AOF segments have the same helical handedness, and to a PM conformer where the two AOF segments have opposite handedness. Indeed, the inversion of handedness for a pentameric helix is expected to be slow on the NMR timescale, whereas the dynamics around the vinylene group (Figure 2a) has been shown above to be fast. The strong bias in favor of one conformer reflects a close-to-quantitative chirality communication between the two helical segments via either a conservation or inversion of helicity.

Slow diffusion of MeOH to a $CHCl_3$ solution of **19** yielded crystals suitable for single crystal X-ray diffraction analysis. The solid state structure of **19** revealed a racemic PP/MM conformation (Figure 3b) in which the vinylene group is in a type II conformation, as observed in the solid state structure of dimer **6**. The dihedral angle between the quinoline rings connected to the vinyl group was measured at 17.5° as the helical twist forbids a planar conformation. In order to assess whether this solid state conformation corresponds to the major species in solution, a ^{1}H NMR spectrum was recorded immediately after dissolving a crystal in $CDCl_3$. Unfortunately, the spectrum showed the two species, indicating that equilibrium had been reached within the time frame of the measurement, that is, more than two minutes. To further slow down the inversion of helix handedness, oligomer **19′** was prepared. This compound comprised two AOF segments containing not 5 but 9 quinoline units linked by one vinyl group. The ^{1}H NMR spectrum of this oligomer also demonstrated two species in the same proportions as **19** (91% and 9%, respectively). Compound **19′** could be crystalized as well and X-ray diffraction analysis revealed a similar conformation to that of **19** (Figure S7). After dissolving a crystal of **19′** in $CDCl_3$, immediate recording of a

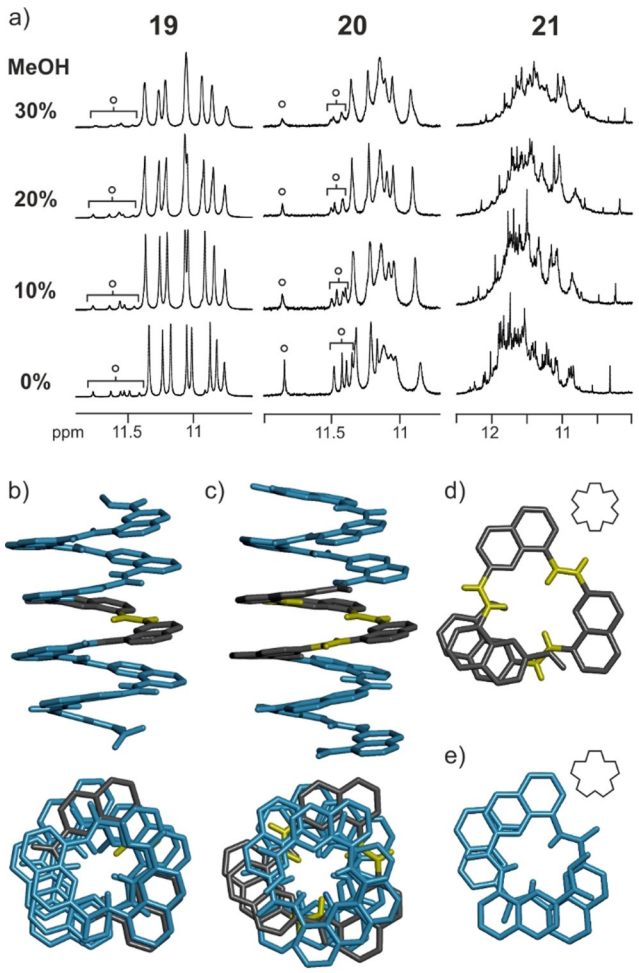

Figure 3. a) Part of the ^{1}H NMR spectra (300 MHz) of **19**, **20** and **21** in $CDCl_3$ containing different proportions of CD_3OH. Empty circles in spectra of **19** and **20**, indicate the coexistence of a second conformer for these compounds. The spectra of **21** showed too many conformers to be identified. b, c) X-ray structures of **19** (b) and **20** (c). d, e) Comparison of the helix cross sections of **20** in its vinylic part (d) and its oligoamide part (e). Side chains and aromatic hydrogen atoms are removed for clarity; vinylene groups are highlighted in yellow. In d), the shape of an 18-crown-6 (top right) highlights the inner rim of the helix in the vinylic part. In e), the shape of an 15-crown-5 (top right) highlights the inner rim of the helix in the amide part.

^{1}H NMR spectrum showed only one set of signals corresponding to the major set at equilibrium. The second set of signals slowly emerged upon the course of hours at 298 K (Figure S9). Thus the match between the major species in solution and the solid state structure was unambiguously established for what concerns the AOF segments.

However, this did not reveal the conformation of the vinylene group, as a rapid equilibrium between conformer II observed in the solid state and conformer IV, both conducive of a helical conformation, could not be excluded. To address this point, ^{1}H–^{1}H NOESY NMR spectra of **19** were recorded as performed for **6**. At 298 K in $CDCl_3$ or CD_2Cl_2, the vinyl proton signals were broad and difficult to assess. When changing the solvent for $C_2D_2Cl_4$ and increasing the temperature to 333 K, two sharp doublets arose at 4.72 and 7.80 ppm corresponding to H^{β} and H^{α}, respectively (Figures S5–S6). The broadness of these

signals at 298 K is indicative of some conformational dynamics around these protons that are neither fast nor slow, including a possible exchange between two conformers. After assigning the aromatic H^3 and H^7 protons adjacent to the vinyl group, NOE correlation cross peaks could be interpreted as being between the signal of H^β and the signals of H^3 and H^7 (Figure S8), showing that conformation II is predominant in solution at this temperature. This result is in sharp contrast with the solution behavior of **6** for which conformer III prevails in solution. It shows that the AOF segments template the conformation of the vinyl bond eventually leading to a canonical helix from a hybrid sequence.

With this result, we investigated the solution behavior of oligomers **20** and **21**, which possess three and five vinyl groups, respectively. As for **19**, the ^{1}H NMR spectrum of compound **20** showed the coexistence of two sets of signals that were attributed to the PP/MM and the PM conformers, in slow exchange on the NMR time scale. The minor species was more abundant than for **19** but its proportion could also be reduced upon adding CD_3OH (Figure 3a). X-ray diffraction analysis of a single crystal of **20** obtained by slow diffusion of MeOH into a CH_2Cl_2 solution also showed a PP/MM canonical helix where all the vinylene bonds adopt conformation II (Figure 3c). In this case the quinolylene–vinylene segment spans a full helix turn. Interestingly, viewing this segment from the top (Figure 3d, e) highlights that its curvature is reduced compared to that of the AOF helix. Bond angles at the amide and vinyl groups differ slightly so that the inner rim of the quinolylene–vinylene segment matches with the shape of an 18-crown-6 macrocycle whereas the inner rim of the AOF helix matches with the shape of a 15-crown-5 macrocycle (Figure 3). The higher curvature of the AOF helix is consequential of a pinching effect within five-membered 2-quinolinecarboxamide hydrogen-bonded rings. The vinylic protons do not form hydrogen bonds strong enough for this pinching to occur and, in that respect, the vinyl group does not constitute a perfect amide isostere.

For compound **21**, analysis of the NMR spectra in $CDCl_3$ revealed a complex behavior with the presence of more than two species. We hypothesized that the pentameric quinolylene–vinylene central segment of **21** adopts several conformations that are no longer in fast exchange as for compounds **6**–**11**. The terminal AOF helices thus slow down conformational dynamics and act as reporters of the different conformations present in solution. Adding CD_3OH (Figure 3a), changing the solvent from $CDCl_3$ to CD_2Cl_2, or heating at 100 °C in $C_2D_2Cl_4$ (Figures S10 and S11) again led to simplifications of the NMR spectrum, but not to the extent that the assignment of a prevailing species could be made. It is thus not clear whether the co-existing conformers are all of type II and IV, that is, conducive of a one handed-helix, or whether the conformers I and III are also present. In any case, the behavior of oligomer **21** suggests that aromatic helices may not be used to template helical folding of more than three vinyl groups.

Conclusions

In this study we have successfully synthetized novel conjugated quinolylene–vinylene oligomer analogs of known oligoamide foldamers that have been previously shown to form a stable helical architecture. These isosteric oligomers did not show a similar propensity to fold into define helical structures. Contrary to their parent molecules, they tend to preferentially adopt an extended conformation in solution. However, we have also demonstrated that helical folding could be templated by the use of short oligoamide segments at each end of the oligomers, if the vinylene segment has up to three vinyl groups. This effect can be further improved by the addition of a polar solvent such as methanol which contributes to solvophobic induced folding. For this new class of hybrid oligomers it is expected that the replacement of the amide groups with vinylene groups not only changes the structural dynamics of the molecules but also their intrinsic properties. As in conducting polymers, the conjugation imparted by vinylene linkages will probably affect the electronic properties of the oligomer. Investigations of the charge transport properties of these compounds are in progress and will be reported in due course.

Experimental Section

General

All chemicals were used as received from commercial sources without further purification unless otherwise specified. Anhydrous THF was obtained from distillation over sodium/benzophenone. Chloroform and diisopropylethylamine were distilled from calcium hydride before using. ^{1}H NMR, ^{13}C NMR and 2D NMR and variable temperature spectra were recorded on BRUKER AVANCE 300 MHz or 400 MHz spectrometers. Chemical shifts are presented in parts per million (δ, ppm) using solvent residue peaks as references (chloroform $\delta = 7.26$ ppm, dichloromethane $\delta = 5.32$ ppm, acetone $\delta = 2.05$ ppm). Coupling constants are reported in Hertz. ESI high resolution mass spectra were recorded on ThermFisher Exactive spectrometer.

General procedure for the synthesis of methylene alcohols

To a 100 mL flask was added the corresponding methyl ester (1 equiv.) and $NaBH_4$ (10 equiv.), then THF was added. The resulting mixture was heated at 50 °C. Methanol was added slowly into the mixture. After complete addition of methanol, the mixture was stirred at 50 °C and the reaction was monitored by TLC. Upon completion of the reaction (usually within one hour), the mixture was allowed to cool to room temperature. Water was added to quench the unreacted $NaBH_4$. Then dichloromethane was added to extract the compound (3×15 mL) and the organic phase was combined and washed with brine. The organic layer was dried over anhydrous Na_2SO_4. The salt was filtrated off and the solvent was removed to give a solid. The product was usually pure enough as indicated by ^{1}H NMR spectra and was used for next step without further purification.

General procedure for the preparation of aldehydes

To a 50 mL flask was added the corresponding methylene alcohol (1 equiv.) and SIBX (1.2 equiv.). Then the flask was equipped with

condenser and magnetic stirring bar. The atmosphere inside the flask was replaced with N_2. Dry THF (15 mL) was added into the flask through a syringe. The mixture was heated under reflux for 1 hour under N_2. Upon completion of the reaction, the reaction was cooled down to room temperature. A saturated aqueous solution of $Na_2S_2O_3$ (10 mL) was added to quench the reaction. Dichloromethane was added to extract the compound and then the organic phase was combined. The organic phase was washed three times with saturated Na_2CO_3 solution. The organic layer was dried over Na_2SO_4 and then filtrated to remove the salt. The solvent was evaporated to give a slurry. Hexane was added to precipitate the compound. The precipitate was filtrated and washed three times with hexane. The solid was collected and dried under vacuum to give the aldehyde.

Synthesis of 4: To a 100 mL flask was added **1** (2.10 g, 7.0 mmol), NBS (1.37 g, 7.7 mmol) and AIBN (22 mg, 0.14 mmol). The air inside the flask was replaced with N_2. Then 40 mL of CCl_4 was added through a syringe. The mixture was heated under N_2 at 75 °C overnight. The reaction mixture was cooled down to room temperature and washed with brine three times. The organic layer was dried over Na_2SO_4, the salt was removed by filtration. The solvent was evaporated to give a slurry. Cyclohexane was added and white needle crystals slowly formed upon standing the solution at room temperature. The solid was filtrated and washed three times with cyclohexane. The solid was collected and dried under vacuum to obtain a white solid (1.85 g, 69.0 %). ^{1}H NMR (300 MHz, $CDCl_3$): δ 8.21 (dd, J = 8.4, 1.5 Hz, 1 H), 7.90 (dd, J = 7.2, 1.5 Hz, 1 H), 7.58 (s, 1 H), 7.56 (t, J = 7.7 Hz, 1 H), 5.31 (s, 2 H), 4.18 (d, J = 5.6 Hz, 2 H), 4.06 (s, 3 H), 1.86 (m, 1 H), 1.64–1.53 (m, 4 H), 0.99 (t, J = 7.4 Hz, 6 H) ppm; ^{13}C NMR (75 MHz, $CDCl_3$): δ 166.5, 163.0, 148.8, 146.0, 137.0, 131.7, 127.2, 122.6, 101.0, 71.1, 53.1, 40.8, 29.5, 23.6, 11.3 ppm, ESI HRMS *m/z*: calcd for $C_{18}H_{23}BrNO_3$ $[M+H]^+$ 380.0856, found 380.0852.

Synthesis of 5: To a 50 mL flask was added **4** (2.36 g, 6.2 mmol). The air inside the flask was replaced with N_2 and triisopropylphosphite (3.0 mL, 12.4 mmol) was added. The mixture was heated at 70 °C for 3 hours under N_2. The reaction mixture was cooled down to room temperature. Toluene was added to remove the excess of triisopropylphosphite by co-evaporating under reduced pressure. The slurry was dried under high vacuum to give a white solid (2.52 g, quant). ^{1}H NMR (300 MHz, $CDCl_3$): δ 8.13 (d, J = 8.5 Hz, 1 H), 7.93 (dd, J = 7.3, 3.4 Hz, 1 H), 7.53 (s, 1 H), 7.54 (t, J = 8.2 Hz, 1 H), 4.74–4.63 (m, 2 H), 4.16 (d, J = 5.4 Hz, 2 H), 4.06 (d, J = 22.3 Hz, 2 H), 1.84 (m, 1 H), 1.61–1.53 (m, 4 H), 1.22 (d, J = 6.4 Hz, 6 H), 1.09 (d, J = 6.4 Hz, 6 H), 0.99 (t, J = 7.2 Hz, 6 H) ppm; ^{13}C NMR (75 MHz, $CDCl_3$): δ 163.1, 148.1, 146.9, 146.8, 132.7, 132.6, 131.6, 131.5, 127.2, 127.1, 122.7, 122.6, 120.8, 120.7, 100.6, 70.7, 52.9, 41.0, 29.2, 27.3, 24.2, 23.9, 23.7, 11.4 ppm; ^{31}P NMR (121 MHz, $CDCl_3$): δ 25.2 ppm, ESI HRMS *m/z*: calcd for $C_{24}H_{37}NO_6P$ $[M+H]^+$ 466.2353, found 466.2348.

General procedure for the Horner–Wadsworth–Emmons (HWE) coupling

To a dry 50 mL flask was added the aldehyde (1 equiv.), **5** (1.1 equiv.) and NaH (2 equiv.). The atmosphere inside the flask was replaced with N_2. Dry THF and 15-crown-5 (1 equiv.) were added though syringes. The mixture was stirred at room temperature for 2 hours. Upon completion, the reaction was quenched by adding water and dichloromethane. The compound was extracted with dichloromethane (15 mL × 3) and the organic layer was dried over Na_2SO_4. The salt was filtrated off and the solvent was removed. The residue was dried under high vacuum. To this solid was added K_2CO_3 (1.5 equiv.) and acetone (20 mL). The mixture was stirred at room temperature for about 10 minutes before adding MeI (2 equiv.). The mixture was stirred at room temperature for 5 hours. Water was then added into the mixture to dissolve the salt. Dichloromethane was added to extract the compound (20 mL × 3). The organic layer was combined and was washed with brine three times (15 mL each time). The organic layer was dried with Na_2SO_4 and the salt was filtrated off. The solvent was evaporated to obtain a slurry. The residue was purified with silica gel column chromatography. The pure fraction was collected and the solvent was removed to give the compound as light yellow solid.

General procedure for Boc-amine deprotection

To a dry flask was added the Boc-protected amine compound (1 equiv.). The compound was dissolved in to 3 mL of dry dichloromethane. Trifluoroacetic acid (TFA, 1 mL) was added into the solution. The mixture was stirred at room temperature for 2 hours. Dichloromethane (15 mL) was added to dilute the solution and the solution was washed with water and saturated $NaHCO_3$ aqueous solution three times. The organic layer was dried over anhydrous Na_2SO_4 and the salt was filtrated off. The solvent was removed and the resulting solid was used without any further purification.

General procedure for the acid chloride coupling

To a dry 25 mL flask was added the corresponding carboxylic acid (1 equiv.). Then the flask was sealed with septum and the atmosphere was exchanged to N_2. Dry chloroform (5 mL) was added into the flask to dissolve the solid under N_2. Then oxalyl chloride (when there is no acid sensitive functional group presented, 5 equiv.) or 1-chloro-N,N,2-trimethyl-1-propenylamine (Ghosez's reagent, when acid sensitive functional groups presented, 1.5 equiv.) was added, the mixture was stirred at room temperature under N_2 for 2 hours. Upon completion of the activation, the solvent was removed under high vacuum and the residue was dried under high vacuum for 3 hours. To a separate dry flask was added the corresponding amine (0.95 equiv.). The flask was sealed with septum and the air was exchanged with N_2. Then dry DIPEA (2 equiv.) and 2 mL of dry chloroform was added into the flask. Under N_2 atmosphere, the acid chloride was removed from the vacuum and dissolved into minimum amount of dry chloroform. The acid chloride solution was transferred into the flask with amine and the resulting mixture was stirred at room temperature under N_2, overnight. Then the reaction was quenched by adding water. Dichloromethane was added to extract the compound. Depending on the purity of the crude, either precipitation with methanol or silica gel column chromatography was used to purify the compound.

Acknowledgements

The China Scholarship Council is gratefully acknowledged for a predoctoral fellowship to J.W. This work benefited from the facilities and expertise of the Biophysical and Structural Chemistry platform at IECB, CNRS UMS3033, INSERM US001, Université de Bordeaux. We thank Dr. B. Kauffmann for assistance with crystallographic measurements. Open access funding enabled and organized by Projekt DEAL.

Conflict of interest

The authors declare no conflict of interest.

Keywords: conformation analysis · foldamers · helices · hybrid sequences · isosteres

[1] G. A. Patani, E. J. LaVoie, *Chem. Rev.* **1996**, *96*, 3147 – 3176.

[2] a) J. Gante, *Angew. Chem. Int. Ed. Eng.* **1994**, *33*, 1699 – 1720; *Angew. Chem.* **1994**, *106*, 1780; b) A. Choudhary, R. T. Raines, *ChemBioChem* **2011**, *12*, 1801 – 1807.

[3] a) N. Dai, F. A. Etzkorn, *J. Am. Chem. Soc.* **2009**, *131*, 13728 – 13732; b) N. Dai, X. J. Wang, F. A. Etzkorn, *J. Am. Chem. Soc.* **2008**, *130*, 5396 – 5397; c) R. R. Gardner, G.-B. Liang, S. H. Gellman, *J. Am. Chem. Soc.* **1995**, *117*, 3280 – 3281.

[4] M. M. Vasbinder, E. R. Jarvo, S. J. Miller, *Angew. Chem. Int. Ed.* **2001**, *40*, 2824 – 2827; *Angew. Chem.* **2001**, *113*, 2906 – 2909.

[5] a) T. Narumi, R. Hayashi, K. Tomita, K. Kobayashi, N. Tanahara, H. Ohno, T. Naito, E. Kodama, M. Matsuoka, S. Oishi, N. Fujii, *Org. Biomol. Chem.* **2010**, *8*, 616 – 621; b) S. Oishi, H. Kamitani, Y. Kodera, K. Watanabe, K. Kobayashi, T. Narumi, K. Tomita, H. Ohno, T. Naito, E. Kodama, M. Matsuoka, N. Fujii, *Org. Biomol. Chem.* **2009**, *7*, 2872 – 2877.

[6] P. Wipf, J. Xiao, C. R. J. Stephenson, *Chim. Int. J. Chem.* **2009**, *63*, 764 – 775.

[7] a) S. H. Gellman, *Acc. Chem. Res.* **1998**, *31*, 173 – 180; b) G. Guichard, I. Huc, *Chem. Commun.* **2011**, *47*, 5933 – 5941; c) D.-W. Zhang, X. Zhao, J.-L. Hou, Z.-T. Li, *Chem. Rev.* **2012**, *112*, 5271 – 5316; d) Y. Zhang, Y. Zhong, A. L. Connor, D. P. Miller, R. Cao, J. Shen, B. Song, E. S. Baker, Q. Tang, S. V. Pulavarti, R. Liu, Q. Wang, Z.-L. Lu, T. Szyperski, H. Zeng, X. Li, R. D. Smith, E. Zurek, J. Zhu, B. Gong, *J. Am. Chem. Soc.* **2019**, *141*, 14239 – 14248; e) M. Pasco, C. Dolain, G. Guichard, *Supramolecular Chemistry in Water* (Ed.: S. Kubik), Wiley-VCH, Weinheim, **2019**, pp. 337 – 374.

[8] a) H. Jiang, J.-M. Léger, I. Huc, *J. Am. Chem. Soc.* **2003**, *125*, 3448 – 3449; b) L. Sebaoun, V. Maurizot, T. Granier, B. Kauffmann, I. Huc, *J. Am. Chem. Soc.* **2014**, *136*, 2168 – 2174; c) M. Jewginski, T. Granier, B. Langlois d'Estaintot, L. Fischer, C. D. Mackereth, I. Huc, *J. Am. Chem. Soc.* **2017**, *139*, 2928 – 2931; d) Y. Ferrand, I. Huc, *Acc. Chem. Res.* **2018**, *51*, 970 – 977.

[9] a) B. Gong, *Acc. Chem. Res.* **2008**, *41*, 1376 – 1386; b) P. Prabhakaran, V. G. Puranik, J. N. Chandran, P. R. Rajamohanan, H.-J. Hofmann, G. J. Sanjayan, *Chem. Commun.* **2009**,3446 – 3448; c) G. M. Burslem, A. J. Wilson, *Synlett* **2014**, *25*, 324 – 335; d) D.-W. Zhang, W.-K. Wang, Z.-T. Li, *Chem. Rec.* **2015**, *15*, 233 – 251; e) I. Arrata, C. M. Grison, H. M. Coubrough, P. Prabhakaran, M. A. Little, D. C. Tomlinson, M. E. Webb, A. J. Wilson, *Org. Biomol. Chem.* **2019**, *17*, 3861 – 3867; f) J. Shen, R. Ye, A. Romanies, A. Roy, F. Chen, C. Ren, Z. Liu, H. Zeng, *J. Am. Chem. Soc.* **2020**, *142*, 10050 – 10058; g) C. Adam, L. Faour, V. Bonnin, T. Breton, E. Levillain, M. Sallé, C. Gautie, D. Canevet, *Chem. Commun.* **2019**, *55*, 8426 – 8429; h) I. Saraogi, A. D. Hamilton, *Chem. Soc. Rev.* **2009**, *38*, 1726 – 1743.

[10] a) H. Jiang, J.-M. Léger, C. Dolain, P. Guionneau, I. Huc, *Tetrahedron* **2003**, *59*, 8365 – 8374; b) C. Dolain, A. Grélard, M. Laguerre, H. Jiang, V. Maurizot, I. Huc, *Chem. Eur. J.* **2005**, *11*, 6135 – 6144; c) T. Qi, V. Maurizot, H. Noguchi, T. Charoenraks, B. Kauffmann, M. Takafuji, H. Ihara, I. Huc, *Chem. Commun.* **2012**, *48*, 6337 – 6339.

[11] a) A. M. Abramyan, Z. Liu, V. Pophristic, *Chem. Commun.* **2016**, *52*, 669 – 672; b) Z. Liu, A. M. Abramyan, V. Pophristic, *New J. Chem.* **2015**, *39*, 3229 – 3240.

[12] a) J. Buratto, C. Colombo, M. Stupfel, S. J. Dawson, C. Dolain, B. Langlois dEstaintot, L. Fischer, T. Granier, M. Laguerre, B. Gallois, Ivan Huc, *Angew. Chem. Int. Ed.* **2014**, *53*, 883 – 887; *Angew. Chem.* **2014**, *126*, 902 – 906; b) K. Ziach, C. Chollet, V. Parissi, P. Prabhakaran, M. Marchivie, V. Corvaglia, P. P. Bose, K. Laxmi-Reddy, F. Godde, J.-M. Schmitter, S. Chaignepain, P. Pourquier, I. Huc, *Nat. Chem.* **2018**, *10*, 511 – 518; c) P. Sai Reddy, B. Langlois d'Estaintot, T. Granier, C. D. Mackereth, L. Fischer, I. Huc, *Chem. Eur. J.* **2019**, *25*, 11042 – 11047.

[13] a) M. Wolffs, N. Delsuc, D. Veldman, N. Vân Anh, R. M. Williams, S. C. J. Meskers, R. A. J. Janssen, I. Huc, A. P. H. J. Schenning, *J. Am. Chem. Soc.* **2009**, *131*, 4819 – 4829; b) X. Li, N. Markandeya, G. Jonusauskas, N. D. McClenaghan, V. Maurizot, S. A. Denisov, I. Huc, *J. Am. Chem. Soc.* **2016**, *138*, 13568 – 13578; c) A. Méndez-Ardoy, N. Markandeya, X. Li, Y.-T. Tsai, G. Pecastaings, T. Buffeteau, V. Maurizot, L. Muccioli, F. Castet, I. Huc, D. M. Bassani, *Chem. Sci.* **2017**, *8*, 7251 – 7257.

[14] a) J. H. Burroughes, D. D. C. Bradley, A. R. Brown, R. N. Marks, K. Mackay, R. H. Friend, P. L. Burns, A. B. Holmes, *Nature* **1990**, *347*, 539 – 541; b) M. Stolka, M. A. Abkowitz, *Synth. Met.* **1991**, *43*, 3385 – 3388; c) L. Liao, Yi. Pang, L. Ding, F. E. Karasz, *Macromolecules* **2001**, *34*, 7300 – 7305; d) F. C. Grozema, L. D. A. Siebbeles, *J. Phys. Chem. Lett.* **2011**, *2*, 2951 – 2958; e) I. Rörich, A.-K. Schonbein, D. K. Mangalore, A. H. Ribeiro, C. Kasparek, C. Bauer, N. I. Craciun, P. W. M. Blom, C. Ramanan, *J. Mater. Chem. C* **2018**, *6*, 10569 – 10579.

[15] a) C. Tanase, J. Wildeman, P. W. M. Blom, *Adv. Funct. Mater.* **2005**, *15*, 2011 – 2015; b) H. Huang, N. Zhou, R. P. Ortiz, Z. Chen, S. Loser, S. Zhang, X. Guo, J. Casado, J. T. López Navarrete, X. Yu, A. Facchetti, T. J. Marks, *Adv. Funct. Mater.* **2014**, *24*, 2782 – 2793.

[16] a) M. Hagihara, N. J. Anthony, T. J. Stout, J. Clardy, S. L. Schreiber, *J. Am. Chem. Soc.* **1992**, *114*, 6568 – 6570; b) C. Baldauf, R. Günther, H.-J. Hofmann, *Helv. Chim. Acta* **2003**, *86*, 2573 – 2588; c) C. Baldauf, R. Günther, H.-J. Hofmann, *J. Org. Chem.* **2005**, *70*, 5351 – 5361; d) H. Wu, H. An, S. Mo, T. Kodadek, *Org. Biomol. Chem.* **2017**, *15*, 3255 – 3264; e) R. Misra, S. Dey, R. M. Reja, H. N. Gopi, *Angew. Chem. Int. Ed.* **2018**, *57*, 1057 – 1061; *Angew. Chem.* **2018**, *130*, 1069 – 1073.

[17] a) C.-E. Chou, D. Wang, M. Bagui, J. Hsu, S. Chakraborty, Z. Peng, *J. Lumines.* **2010**, *130*, 986 – 994; b) Y. Chen, Y. Xu, K. Perry, A. P. Sokolov, K. More, Y. Pang, *ACS Macro Lett.* **2012**, *1*, 701 – 705; c) C. De Göen, I. Cianga, L. Cianga, Y. Yagcia, *Design. Monom. Polym.* **2016**, *19*, 508 – 534; d) Z. Zhuang, P. Shen, S. Ding, W. Luo, B. He, H. Nie, B. Wang, T. Huang, R. Hu, A. Qin, Z. Zhao, B. Z. Tang, *Chem. Commun.* **2016**, *52*, 10842 – 10845.

[18] A. Ozanne, L. Pouységu, D. Depernet, B. François, S. Quideau, *Org. Lett.* **2003**, *5*, 2903 – 2906.

[19] T. Qi, T. Deschrijver, I. Huc, *Nat. Prot.* **2013**, *8*, 693 – 708.

[20] H. Nagaoka, Y. Kishi, *Tetrahedron* **1981**, *37*, 3873 – 3888.

[21] a) J.-L. Hou, M.-X. Jia, X.-K. Jiang, Z.-T. Li, G.-J. Chen, *J. Org. Chem.* **2004**, *69*, 6228 – 6237; b) T. V. Jones, M. M. Slutsky, R. Laos, T. F. A. de Greef, G. N. Tew, *J. Am. Chem. Soc.* **2005**, *127*, 17235 – 17240; c) M. T. Stone, J. M. Heemstra, J. S. Moore, *Acc. Chem. Res.* **2006**, *39*, 11 – 20; d) Y. Wang, F. Li, Y. Han, F. Wang, H. Jiang, *Chem. Eur. J.* **2009**, *15*, 9424 – 9433; e) H. H. Nguyen, J. H. McAliley, W. R. Batson, D. A. Bruce, *Macromolecules* **2010**, *43*, 5932 – 5942.

[22] a) D. Sánchez-García, B. Kauffmann, T. Kawanami, H. Ihara, M. Takafuji, M.-H. Delville, I. Huc, *J. Am. Chem. Soc.* **2009**, *131*, 8642 – 8648; b) C. Dolain, J.-M. Léger, N. Delsuc, H. Gornitzka, I. Huc, *Proc. Natl. Acad. Sci. USA* **2005**, *102*, 16146 – 16151; c) M. Kudo, V. Maurizot, B. Kauffmann, A. Tanatani, I. Huc, *J. Am. Chem. Soc.* **2013**, *135*, 9628 – 9631.

Manuscript received: July 30, 2020
Revised manuscript received: September 1, 2020
Accepted manuscript online: September 3, 2020
Version of record online: December 3, 2020